Electronic Supplementary Material (ESI) for Dalton Transactions.

Phosphorescent Cyclometalated Ir(III) Complex-Functionalized Molecularly-Imprinted Polymer for Specific Trimethylamine Detection

Ruoyang Liu[a], Shun-Cheung Cheng[a], Chi-On Ng[a], Yelan Xiao[a,b], Kin-Man Tang[a], Ka-Ming Tong[a], Ngai-Yu Lei[a], Chi-Chiu Ko[a,*]

[a]*Department of Chemistry and State Key Laboratory of Marine Pollution, City University of Hong Kong, Hong Kong, China*

[b]*Shenzhen Key Laboratory for Nano-Biosensing Technology, Research Center for Biosensor and Nanotheranostic, School of Biomedical Engineering, Health Science Center, Shenzhen University, Shenzhen, Guangdong, China*

Email address: vinccko@cityu.edu.hk (C.-C. Ko)

Supplementary Information

Contents

3. References

1. Experimental Section

{Ir(ppy)$_2$[phen(OH)$_2$]}PF$_6$ (Ir-1). ^{1}H NMR (300 MHz, $(CD_3)_2CO$): δ 8.38 (2H, s, 5-, 6-H's of phenathroline), 8.22 (2H, d, *J* = 8.1 Hz, two 6-pyridyl H's of ppy), 7.89 (6H, m, two 3-pyridyl H's of ppy, two 4-pyridyl H's of ppy and two 2-phenyl H's of ppy), 7.80 (2H, d, *J* = 5.7 Hz, 3-, 8- H's of phenathroline), 7.31 (2H, d, *J* = 6.1 Hz, 2-, 9- H's of phenathroline), 7.05 (4H, m, two 3-phenyl H's of ppy and two 4-phenyl H's of ppy), 6.93 (2H, m, two 5-pyridyl H's of ppy), 6.48 (2H, d, *J* = 7.4 Hz, two 5-phenyl H's of ppy), 3.83 (s, 2H, OH). Positive-ion ESI-MS: m/z 713.2 $[M]^+$; IR (KBr disc / cm^{-1}): 3059 br (O-H), 831 (P-F).

{Ir(ppy)$_2$[(OMe)$_2$phen]}PF$_6$ (Ir-2). ^{1}H NMR (300 MHz, $CDCl_3$): δ 8.36 (2H, s, 5-, 6- H's of phenathroline), 8.07 (2H, d, *J* = 6.0 Hz, two 6-pyridyl H's of ppy), 7.89 (2H, d, *J* = 8.3 Hz, 3-, 8- H's of phenathroline), 7.70 (4H, d, *J* = 7.4 Hz, two 3-pyridyl H's of ppy and two 4-pyridyl H's of ppy), 7.50 (2H, d, *J* = 6.1 Hz, two 2-phenyl H's of ppy), 7.16 (2H, d, *J* = 6.1 Hz, 2-, 9- H's of phenathroline), 7.05 (2H, m, two 5-pyridyl H's of ppy), 6.94 (4H, m, two 3-phenyl H's of ppy and two 4-phenyl H's of ppy), 6.41 (2H, d, *J* = 7.5 Hz, two 5-phenyl H's of ppy), 4.19 (6H, s, CH_3). Positive-ion ESI-MS: m/z 741.2 $[M]^+$; IR (KBr disc / cm^{-1}): 846 (P-F).

Physical Measurements and Instrumentation.

Instrumentation for NMR, IR, UV-vis diffuse reflectance, time-resolved emission and Raman spectroscopy, elemental analysis, TGA and ICP-OES are carried out according to our previously reported literature [1,2]. For Raman spectra, excitation beam (309 nm) is produced by a Nd:YAG laser (Spectra-Physics LAB-170). Solvent signals are subtracted and frequencies are calibrated by methanol Raman bands.

The concentrations of TMA·HCl are quantified by LC-MS using Agilent 1200 HPLC equipped with Sciex API 2000 MS/MS system. Ethyl bromoacetate was used to derivatize TMA, to improve ESI-MS/MS detection and separation of TMA. A portion of 125 μL supernatant was mixed with 425 μL of 20% concentrated ammonium solution, triethylamine (TEA) as an internal standard in acetonitrile and 100 μL of 4.0 M ethyl bromoacetate in acetonitrile. The mixture was stand overnight at 25 °C. Thereafter, 250 μL of MeCN/Milli-Q water/HCOOH (50:50:1 v/v/v) was added to terminate the reaction. The solution was ready for LC-MS/MS analysis. The chromatographic separation was performed using a Water HILIC silica column (3 μm, 2.1 × 100 mm) with isocratic elution using 10 mM $HCOONH_4$ in water / 0.1% HCOOH in MeCN (v/v 1:9) as eluent (flow rate: 400 μL/min). The LC-MS calibration curve is shown below:

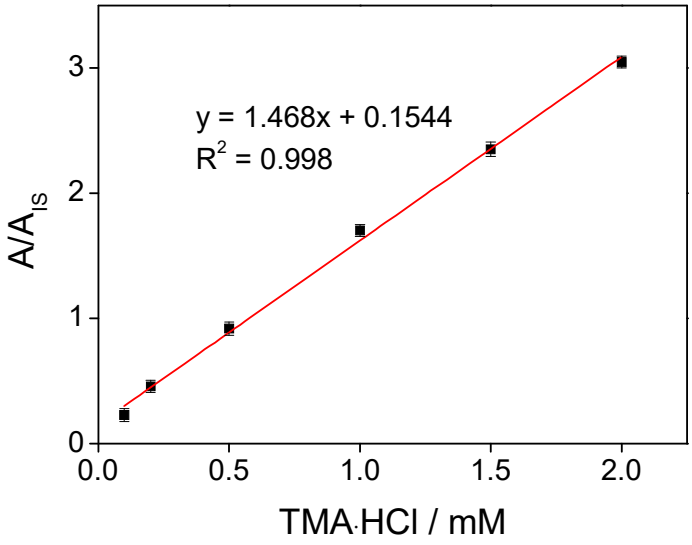

A: Peak area, IS: internal standard, triethylamine

Emission quenching experiments with different concentrations of TMA·HCl are conducted in a quartz cell, degassed by bubbling argon. The quenching rate constants are calculated through the Stern-Volmer equation:

$$\tau_0/\tau = 1 + k_q\tau_0[Q]$$

τ_0 and τ are emission lifetimes without and with quencher, [Q] is quencher concentration in mol $dm^{-3,}$ and k_q is the bimolecular quenching rate constant.

TMA-sensing study

The emission titration was performed on an Edinburgh Instruments FLS980 spectrometer. The **PTMA-Ir** suspended in an aqueous solution was incubated with different concentrations of TMA·HCl for 2 hours, and degassed before the emission measurement. To test the amine vapor sensing, **PTMA-Ir** adsorbed on filter paper (**T-Ir**) was prepared by dipping a filter paper strip (23 mm × 13mm) on a **PTMA-Ir**-suspended solution (1 mg **PTMA-Ir** in 10 mL *n*-hexane). The emission of **PTMA-Ir** on **T-Ir** in a closed quartz cuvette with different concentrations of TMA vapor prepared by the injection of saturated TMA vapor was examined. Saturated TMA vapor is prepared by dissolving TMA·HCl (1 g) in NaOH solution (600 mg NaOH in 10 mL milliQ water) in a closed system at 25 ºC for 3 hours. The injected TMA contents are verified by FT-IR spectroscopy with a 10-cm infrared gas cell according to the peak area at 1459 cm^{-1} as shown in the following figures.

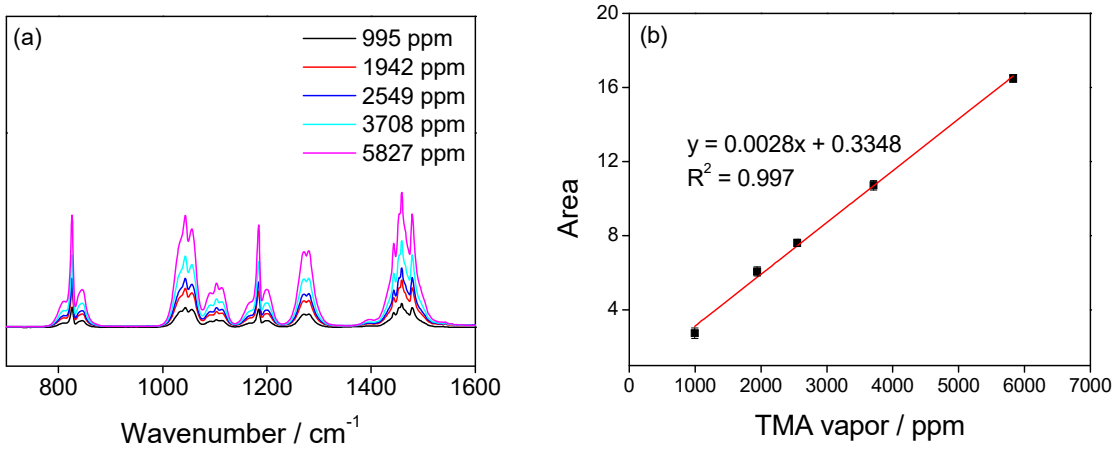

(a) FT-IR spectra and (b) calibration curve of TMA vapor (25 °C).

2. Supplementary figures

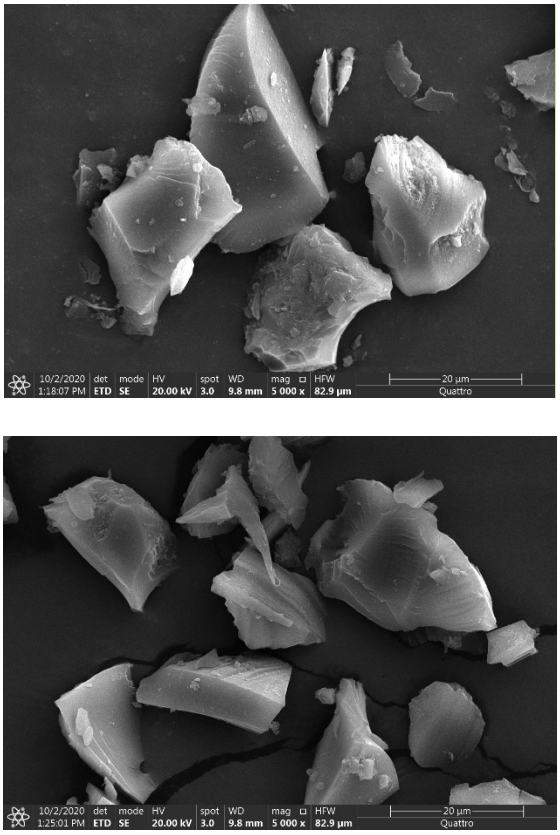

Fig. S1 SEM images of (a) **PTMA** and (b) **PTMA-Ir**.

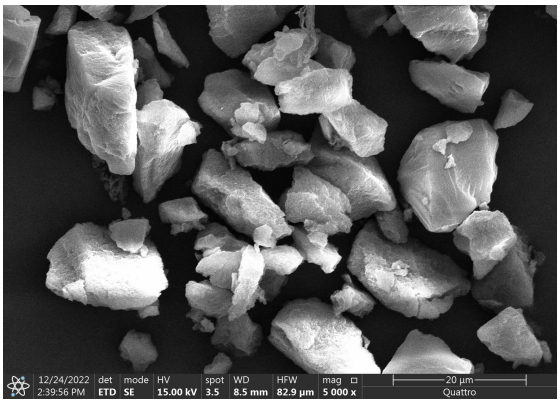

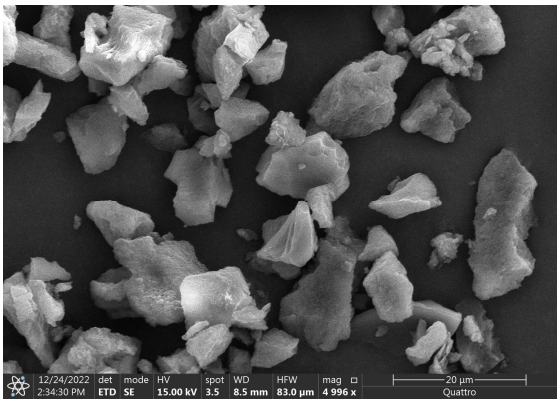

Fig. S2 SEM images of the control polymers without TMA-imprinting cavities (**P** and **P-Ir**) prepared according to identical synthetic procedures for **PTMA** and **PTMA-Ir** except no imprinting template was used in the synthesis.

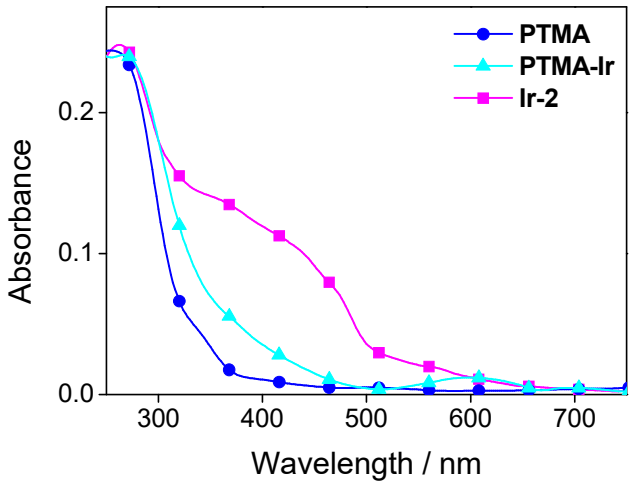

Fig. S3 UV-vis reflectance spectra of **PTMA**, **Ir-2** and **PTMA-Ir** deposited on a quartz plate with a 1-cm circular recess.

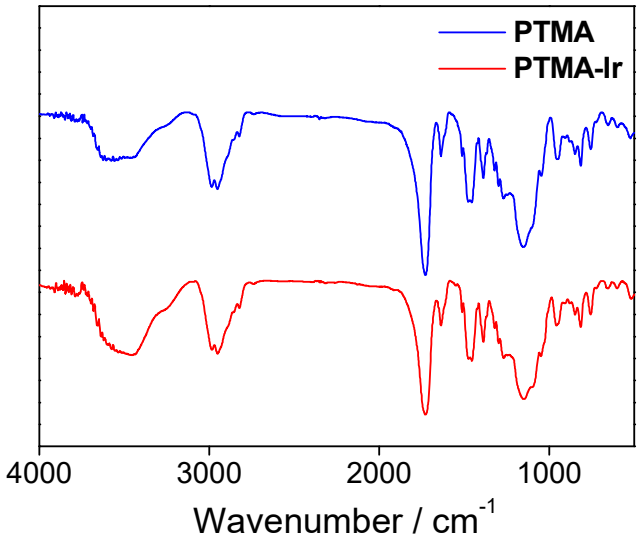

Fig. S4 FT-IR spectra of **PTMA** and **PTMA-Ir**.

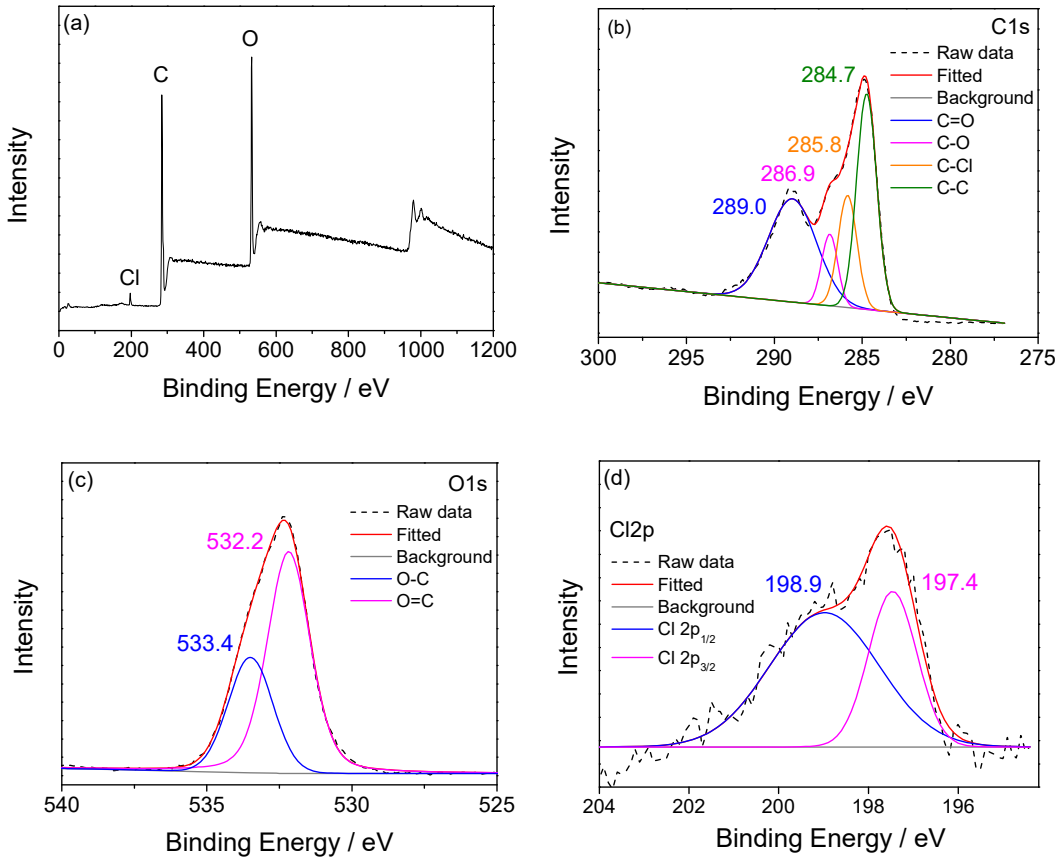

Fig. S5 (a) XPS survey spectrum of **PTMA** and deconvoluted fittings of the high resolution (b) C 1s, (c) O 1s and (d) Cl 2p signals.

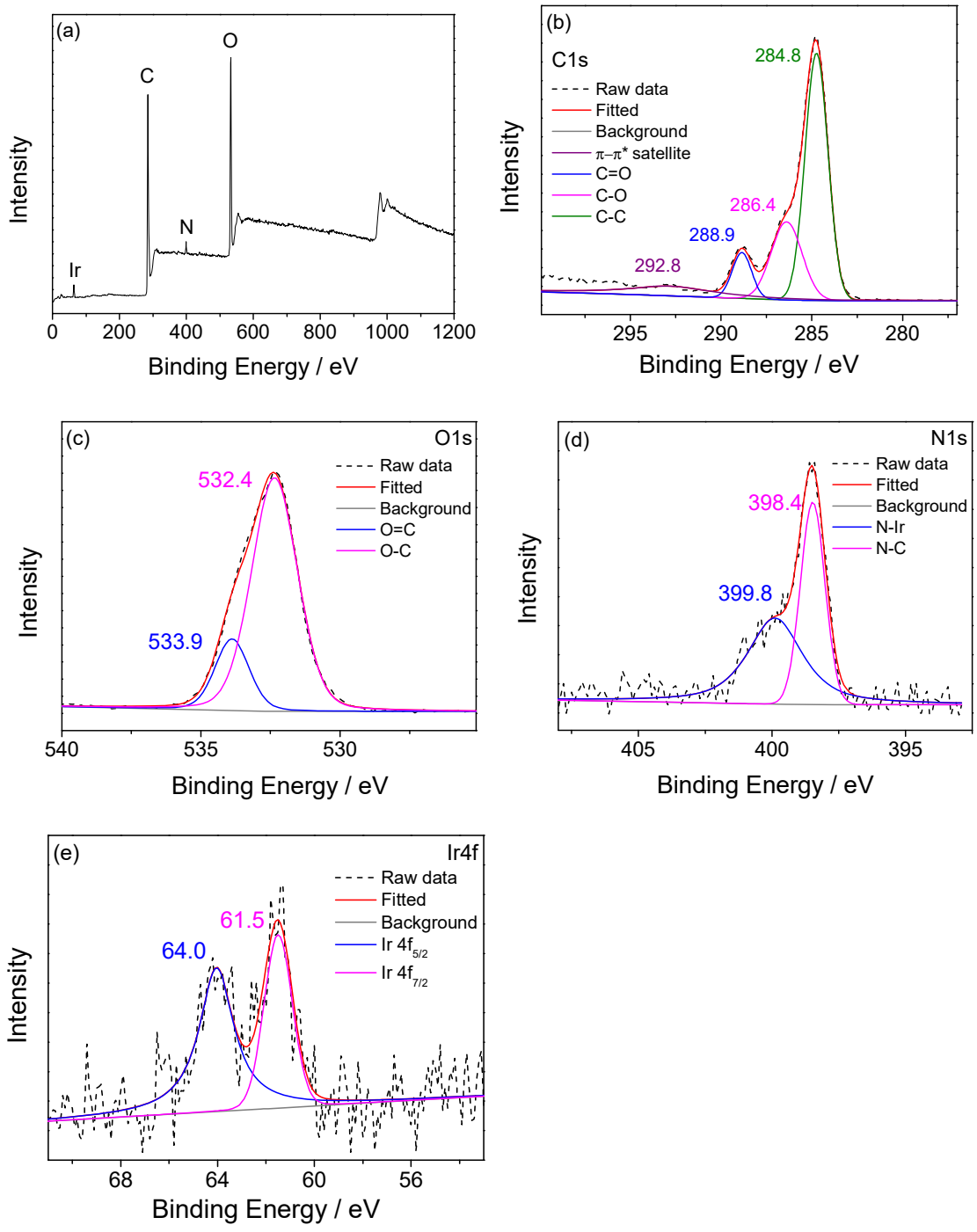

Fig. S6 (a) XPS survey spectrum of **PTMA-Ir** and deconvoluted fittings of the high resolution (b) C 1s, (c) O 1s, (d) N 1s and (e) Ir 4f signals.

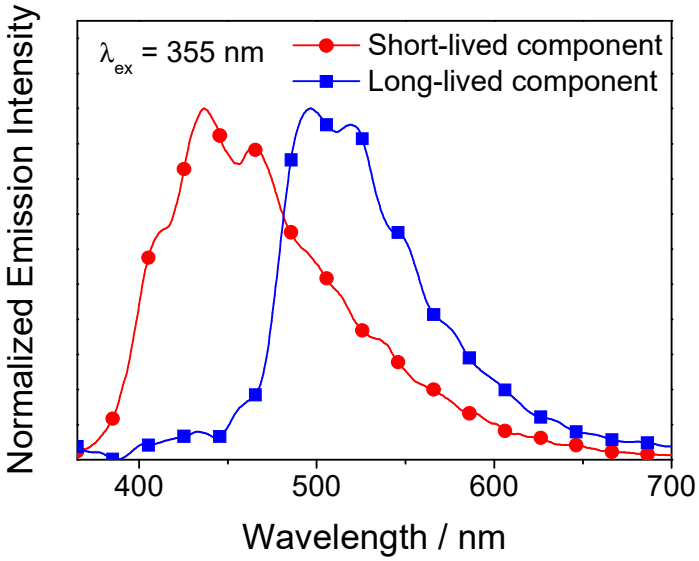

Fig. S7 Nanosecond time-resolved emission spectra of **PTMA-Ir** suspended in H_2O (λ_{ex} = 355 nm).

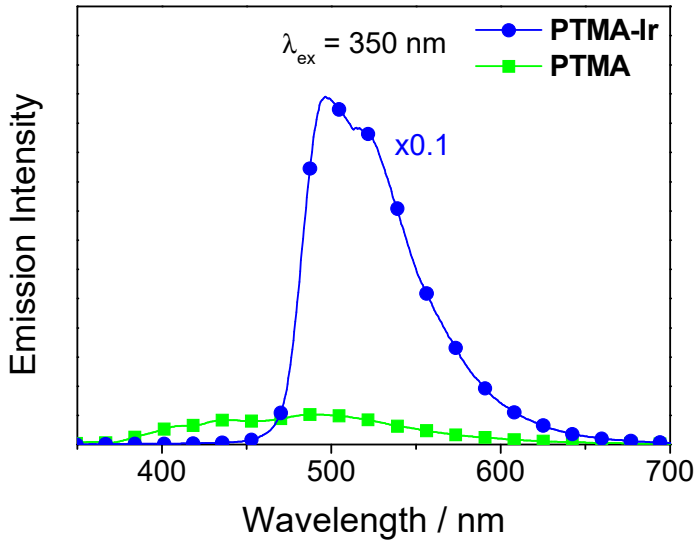

Fig. S8 Overlaid emission spectra of **PTMA-Ir** and **PTMA** suspended in H_2O (0.2 mg polymer in 3 mL H_2O) (λ_{ex} = 350 nm).

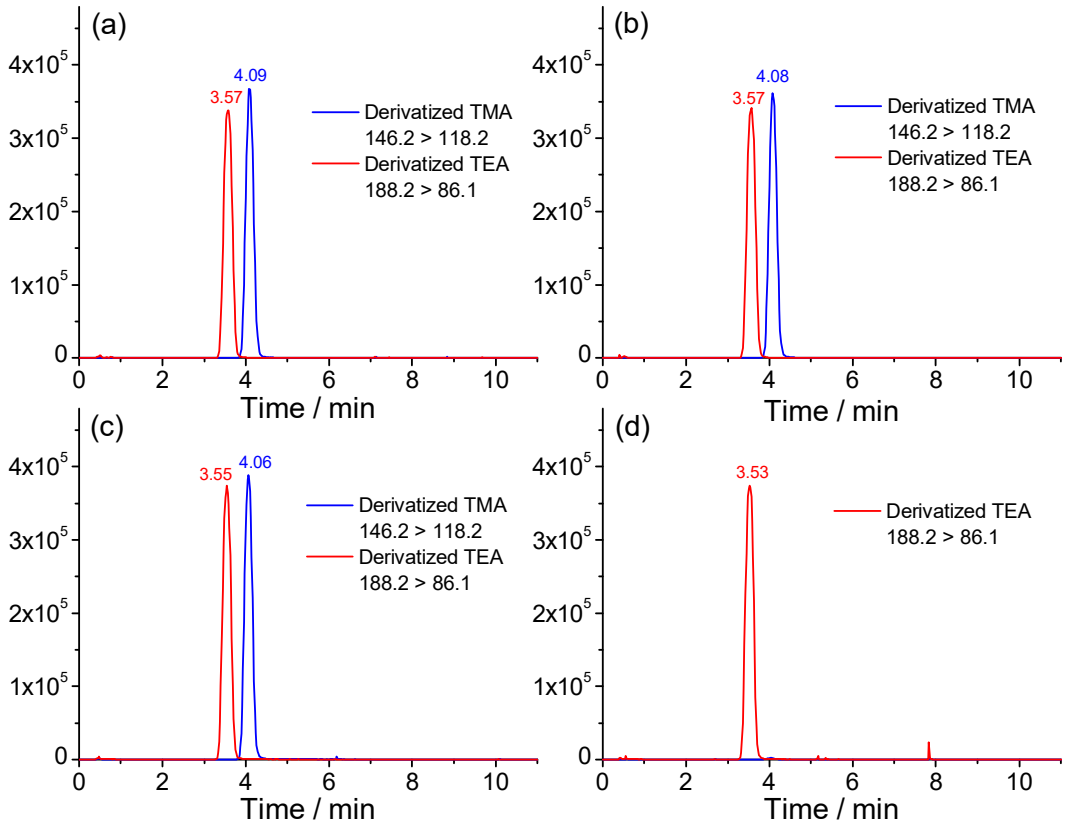

Fig. S9 Extracted-ion chromatograms (XIC) of derivatized TMA and TEA monitored at their specific multiple reaction monitoring (MRM) transitions in the study of **PTMA-Ir**. (a), (b) and (c) are spiked sample replicates, and (d) is the negative control.

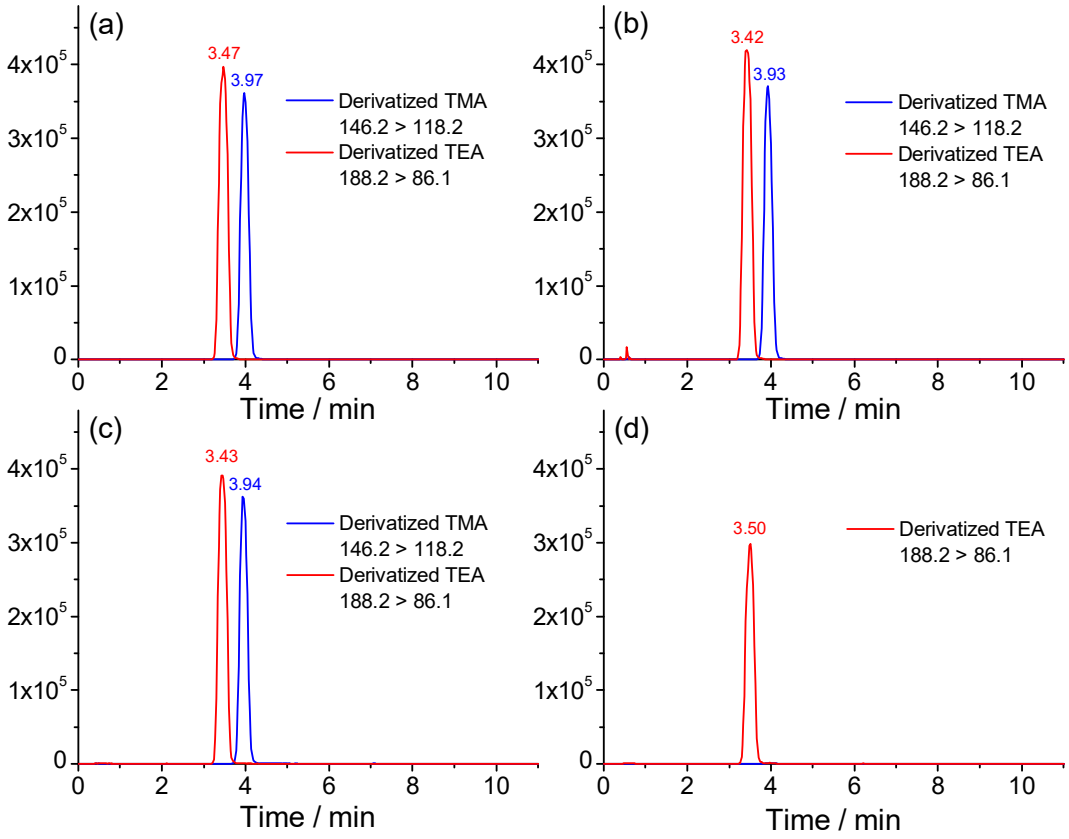

Fig. S10 Extracted-ion chromatograms (XIC) of derivatized TMA and TEA monitored at their specific MRM transitions in the study of **P-Ir**. (a), (b) and (c) are spiked sample replicates, and (d) is the negative control.

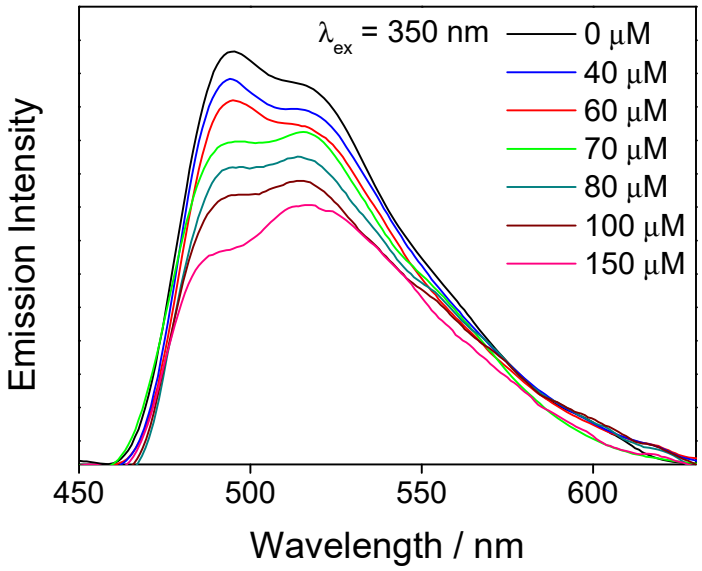

Fig. S11 Emission spectra of **PTMA-Ir** suspended in an acidic aqueous solution (pH = 2) after incubation in different concentrations of TMA·HCl for 120 min (λ_{ex} = 350 nm).

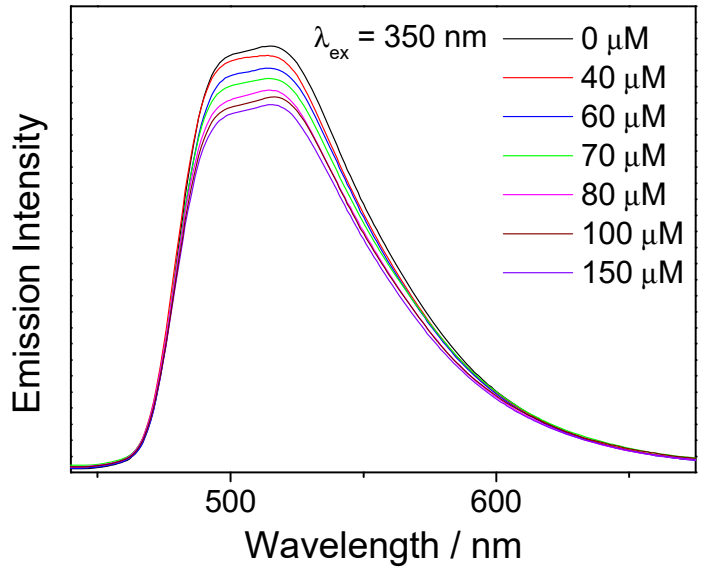

Fig. S12 Emission spectra of **Ir-2** in CH_3CN/H_2O (3:2 v/v) after incubation with different concentrations of TMA·HCl (λ_{ex} = 350 nm).

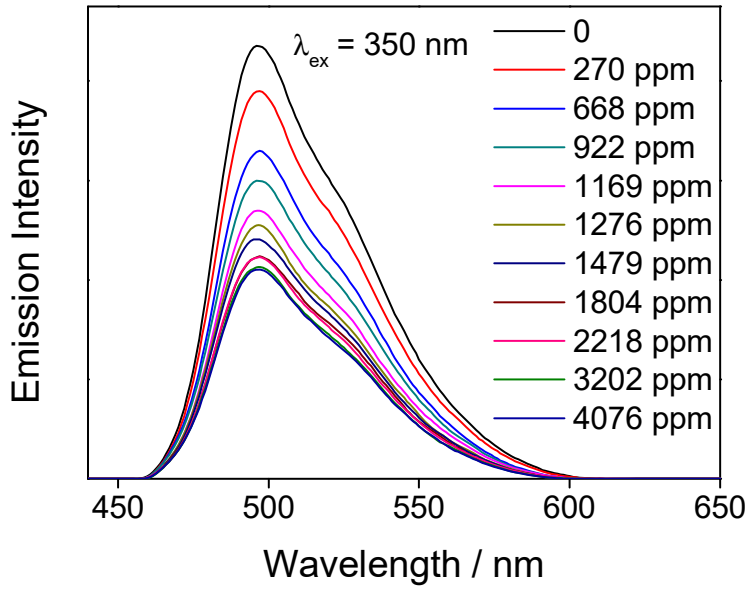

Fig. S13 Emission spectra of **T-Ir** upon exposure to different concentrations of TMA vapor under an air atmosphere (λ_{ex} = 350 nm).

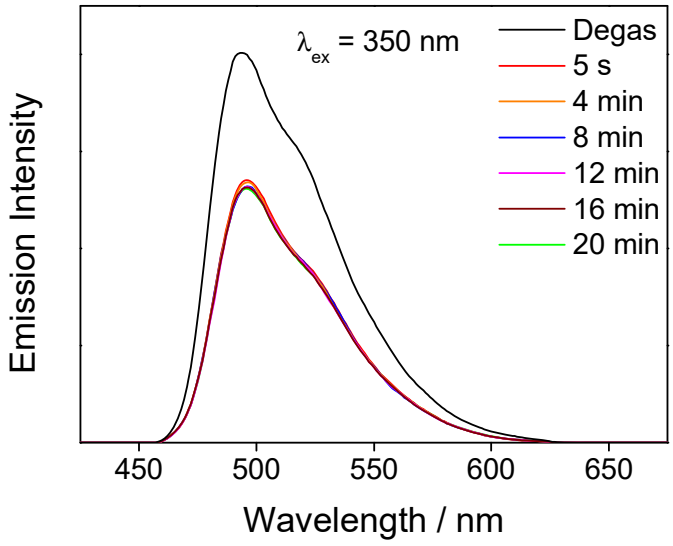

Fig. S14 Time-dependent emission spectra of **PTMA-Ir** under an argon atmosphere upon exposure to 634 ppm TMA vapor (λ_{ex} = 350 nm).

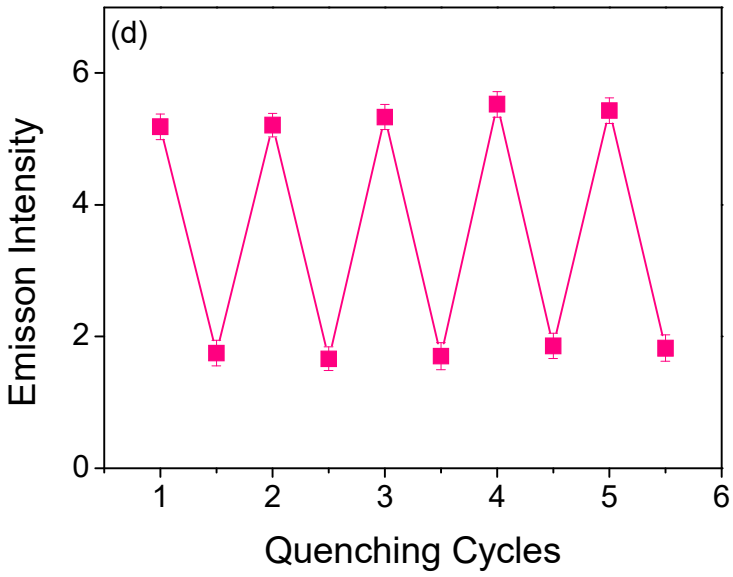

Fig. S15 Emission responses of **T-Ir** under an air atmosphere upon exposure to 1800 ppm of TMA vapor and removal from TMA vapor over five cycles.

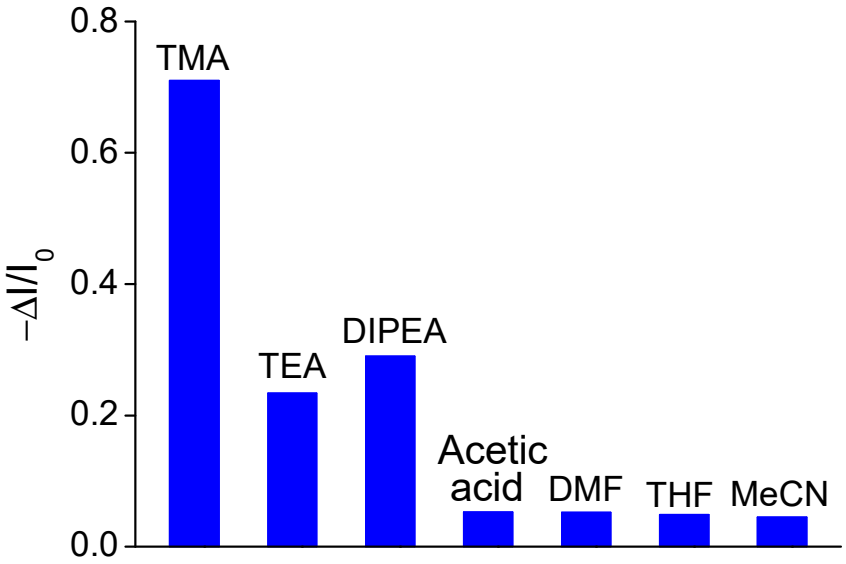

Fig. S16 Emission quenching of **T-Ir** under an argon atmosphere upon exposure to 3950 ppm vapor of TMA and saturated vapor of other interfering reagents at 20 °C [TEA (~75,000 ppm), DIPEA (~14,100 ppm), acetic acid (~14,800 ppm), DMF (~3,800 ppm), THF (~188,000 ppm) and MeCN (~108,600 ppm)].

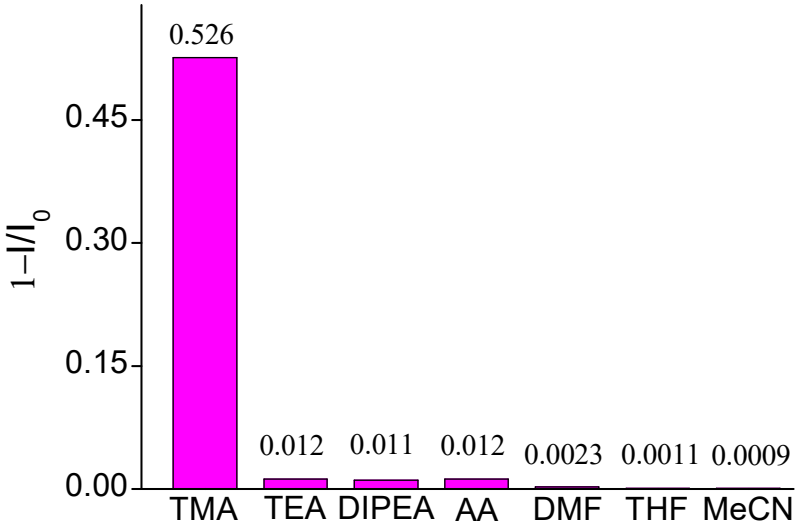

Fig. S17 Emission quenching of **T-Ir** under an air atmosphere upon exposure to 1800 ppm vapor of TMA and other interfering reagents.

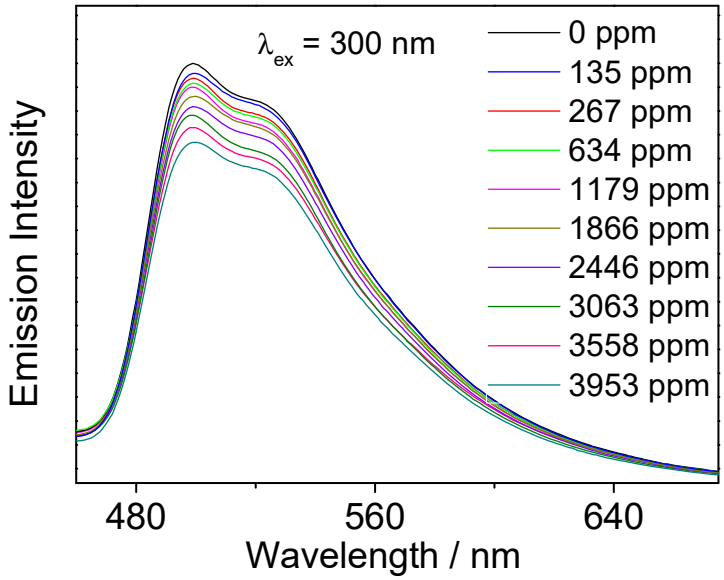

Fig. S18 Emission spectra of **Ir-2** loaded on a filter paper upon exposure to different concentrations of TMA vapor under an argon atmosphere (λ_{ex} = 300 nm).

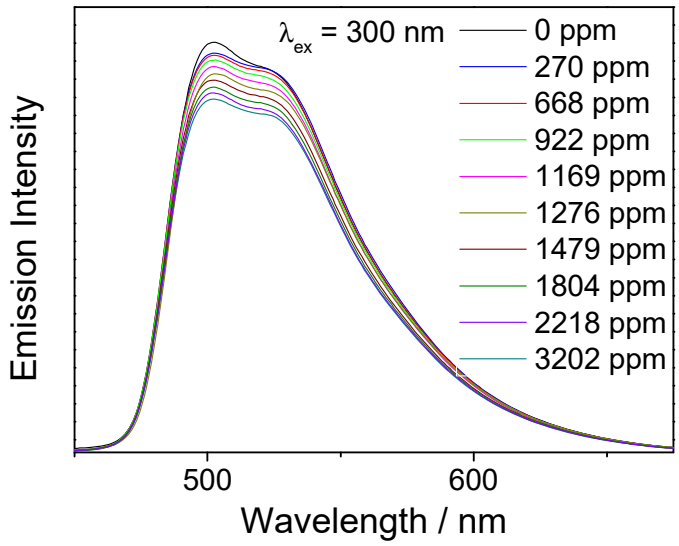

Fig. S19 Emission spectra of **Ir-2** loaded on a filter paper upon exposure to different concentrations of TMA vapor under an air atmophere (λ_{ex} = 300 nm).

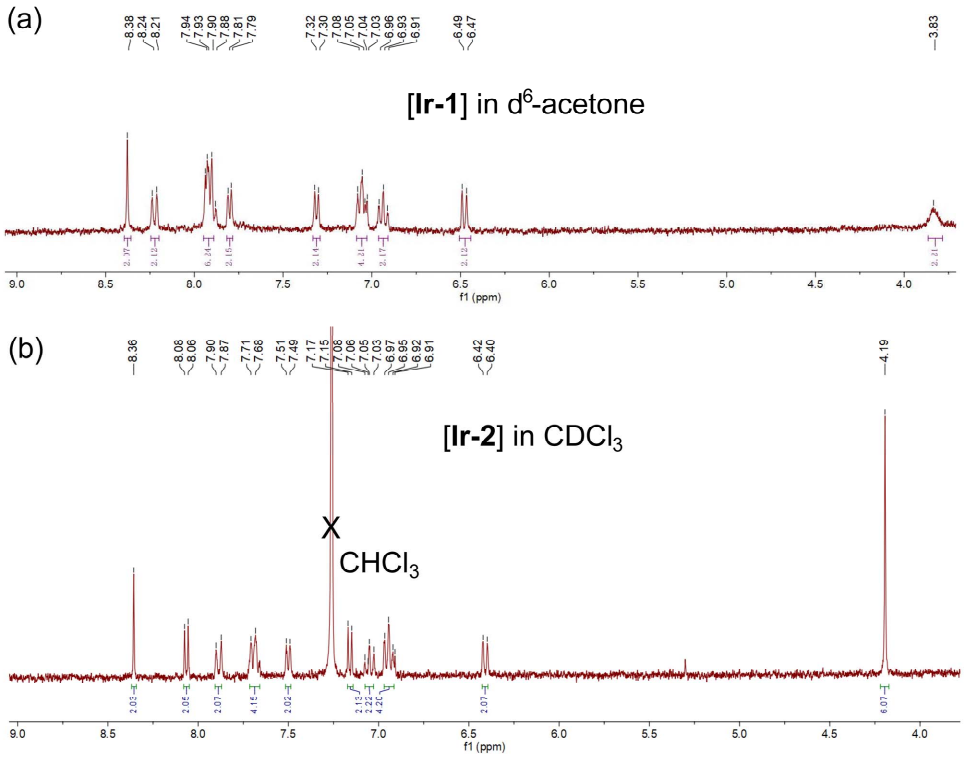

Fig. S20 ^{1}H NMR spectra of (a) [**Ir-1**] in $(CD_3)_2CO$ and (b) [**Ir-2**] in $CDCl_3$.

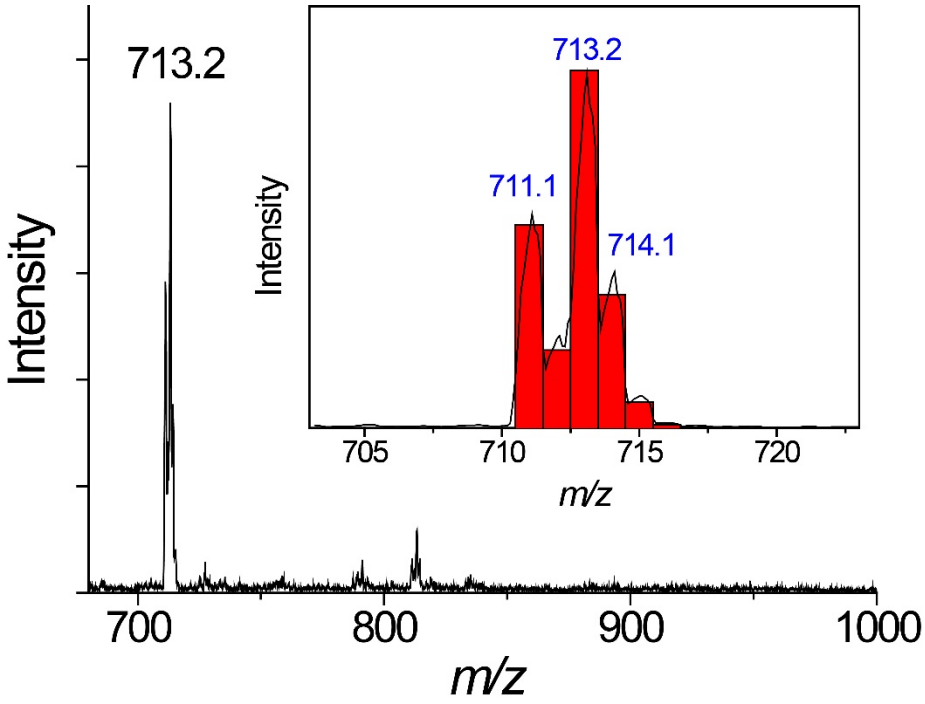

Fig. S21 Positive ESI mass spectrum of [**Ir-1**]. The inset shows the expanded ion cluster at *m/z* = 713.2.

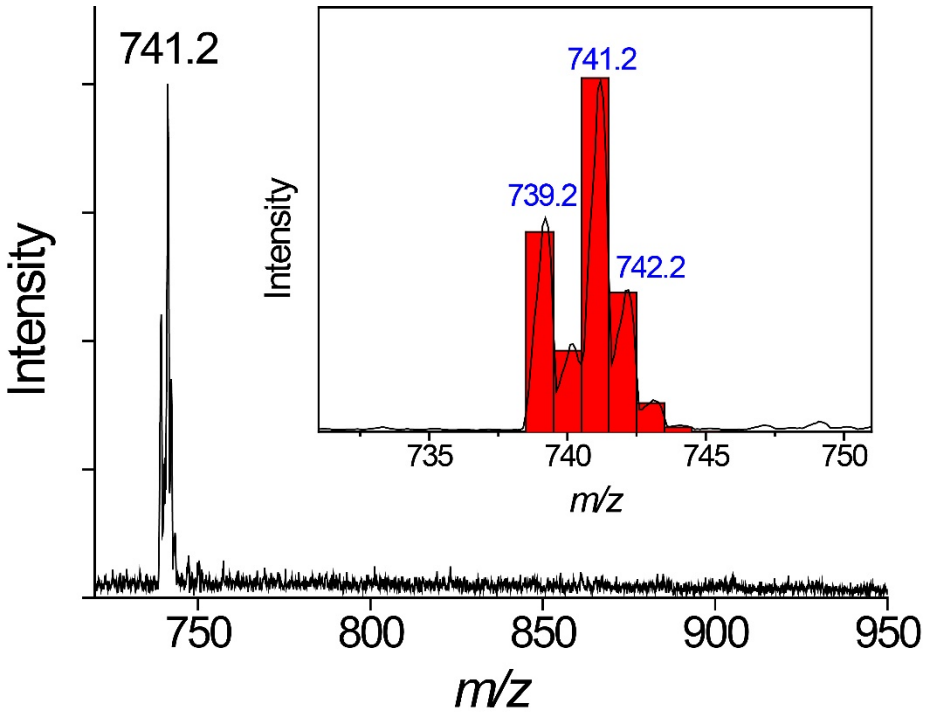

Fig. S22 Positive ESI mass spectrum of [**Ir-2**]. The inset shows the expanded ion cluster at *m/z* = 741.2.

Table S1. Comparison of **PTMA-Ir** sensor with recently reported TMA sensors.

Sensing Material	Sensing Temp. (°C)	Tested Range (ppm)	LOD	Response Time	Ref.
MoO_3	300	0.1 – 1000	0.01 ppm	8 s	[3]
Ru-SnO_2	400	1 – 5	1 ppm	/	[4]
Graphene quantum dots / α-Fe_2O_3	270	0.01 – 1000	0.01 ppm	11 s	[5]
rGO / In_2O_3	RT	100 – 1500	100 ppm	2 s	[6]
α-Fe_2O_3	250	1 – 100	1 ppm	< 1 min	[7]
Au / PdO / $WO_{2.72}$	240	1 – 100	1 ppm	4 s	[8]
Co_3O_4 / ZnO	250	0.33 – 66	130 ppb	3 s	[9]
Au / WO_3	300	0.5 – 25	0.5 ppm	8 s	[10]
PTMA-Ir	25	0 – 1179 0 – 1276	9 ppm 15 ppm	5 s	This work

3. References

[1] Liu, R.; Cheng, S.-C.; Xiao, Y.; Chan, K.-C.; Tong, K.-M.; Ko, C.-C. Recyclable Polymer-Supported Iridium-Based Photocatalysts for Photoredox Organic Transformations. *J. Catal.* **2022**, *407*, 206-212.

[2] Kwok, W. M.; Phillips, D. L.; Yeung, P. K.-Y.; Yam, V. W.-W. Resonance Raman Investigation of the MLCT Transition in $[Pt(dppm)_2(PhC{\equiv}C)_2]$ and the MMLCT Transition in $[Pt_2(\mu\text{-dppm})_2(\mu\text{-PhC}{\equiv}C)(PhC{\equiv}C)_2]^+$, *J. Phys. Chem. A*, **1997**, *101*, 9286–9295.

[3] Chu, X.; Liang, S.; Sun, W.; Zhang, W.; Chen, T.; Zhang, Q. Trimethylamine sensing properties of sensors based on MoO_3 microrods, *Sensors Actuators, B Chem.*, **2010**, *148*, 399–403.

[4] Kim, K.-M.; Choi, K.-Il; Jeong, H.-M.; Kim, H.-J.; Kim, H.-R.; Lee, J. H. Highly sensitive and selective trimethylamine sensors using Ru-doped SnO_2 hollow spheres, *Sensors Actuators, B Chem.*, **2012**, *166–167*, 733–738.

[5] Hu, T.; Chu, X.; Gao, F.; Dong, Y.; Sun, W.; Bai, L. Trimethylamine sensing properties of graphene quantum Dots/α-Fe_2O_3 composites, *J. Solid State Chem.*, **2016**, *237*, 284–291.

[6] Ma, Z.; Song, P.; Yang, Z.; Wang, Q. Trimethylamine detection of 3D rGO/mesoporous In_2O_3 nanocomposites at room temperature, *Appl. Surf. Sci.*, **2019**, *465*, 625–634.

[7] Liu, L.; Fu, S.; Lv, X.; Yue, L.; Fan, L.; Yu, H.; Gao, X.; Zhu, W.; Zhang, W.; Li, X.; Zhu, W. A Gas Sensor With Fe_2O_3 Nanospheres Based on Trimethylamine Detection for the Rapid Assessment of Spoilage Degree in Fish, *Front. Bioeng. Biotechnol.*, **2020**, *8*, 1–9.

[8] Shang, Y.; Shi, R.; Cui, Y.; Che, Q.; Wang, J.; Yang, P. Urchin-Like $WO_{2.72}$ Microspheres Decorated with Au and PdO Nanoparticles for the Selective Detection of Trimethylamine, *ACS Appl. Nano Mater.*, **2020**, *3*, 5554–5564.

[9] Yan, W.; Xu, H.; Ling, M.; Zhou, S.; Qiu, T.; Deng, Y.; Zhao, Z.; Zhang, E. MOF-Derived Porous Hollow Co_3O_4@ZnO Cages for High-Performance MEMS Trimethylamine Sensors, *ACS Sensors*, **2021**, *6*, 2613–2621.

[10] Zhao, C.; Shen, J.; Xu, S.; Wei, J.; Liu, H.; Xie, S.; Pan, Y.; Zhao, Y.; Zhu, Y. Ultra-efficient trimethylamine gas sensor based on Au nanoparticles sensitized WO_3 nanosheets for rapid assessment of seafood freshness, *Food Chem.*, **2022**, *392*, 133318.